

Exact order, gap and counting statistics of a Brownian gas correlated by resetting

Marco Biroli,¹ Hernan Larralde,² Satya N. Majumdar,¹ and Grégory Schehr³

¹LPTMS, CNRS, Univ. Paris-Sud, Université Paris-Saclay, 91405 Orsay, France

²Instituto de Ciencias Fisicas, UNAM, Av. Universidad s/n, CP 62210 Cuernavaca Morelos, Mexico

³Sorbonne Université, Laboratoire de Physique Théorique et Hautes Energies, CNRS UMR 7589, 4 Place Jussieu, 75252 Paris Cedex 05, France

We study a one-dimensional gas of N Brownian particles that diffuse independently, but are *simultaneously* reset to the origin at a constant rate r . The system approaches a non-equilibrium stationary state (NESS) with long-range interactions induced by the simultaneous resetting. Despite the presence of strong correlations, we show that several observables can be computed exactly, which include the global average density, the distribution of the position of the rightmost particle, the spacing distribution between two successive particles and the full counting statistics, i.e., the distribution of the number of particles in a given interval. Our analytical results are confirmed by numerical simulations. We also discuss a possible experimental realisation of this resetting gas using optical traps.

While the properties of a gas of noninteracting particles are well understood, those of an interacting gas, in particular in the presence of a long-range interaction between particles, are much less so. A notable exception is the celebrated Dyson's log-gas in one-dimension, that appears in the spectral statistics of random matrix theory (RMT). Indeed, the statistics of the eigenvalues of Gaussian random matrices play a major role in several areas of science, from nuclear physics, quantum chaos, mesoscopic transport, all the way to finance and information theory [1–4]. For an $N \times N$ matrix (real symmetric, complex Hermitian or quaternionic symplectic) with independent Gaussian entries, the joint probability distribution function (JPDF) of the N real eigenvalues $\{x_i\}$ can be expressed as a Boltzmann weight $P[\{x_i\}] \propto \exp(-\beta E[\{x_i\}])$ with the energy given by $E[\{x_i\}] = \frac{1}{2} \sum_{i=1}^N x_i^2 - \frac{1}{2} \sum_{i \neq j} \ln|x_i - x_j|$, where the Dyson index $\beta = 1, 2, 4$ corresponds to the three symmetry classes mentioned above [1, 2]. Thus, the eigenvalues x_i can be interpreted as the positions of N particles on a line in the presence of a confining harmonic potential, with pairwise logarithmic repulsion between them. This is the Dyson's log-gas [5], which has been a fundamental cornerstone [2] in understanding the role of strong correlations on several spectral observables such as the average density of eigenvalues [6], the spacing distribution between eigenvalues [1, 2, 7], the largest eigenvalue [8–11] (i.e., the position of the rightmost particle in the gas) and the full counting statistics (FCS), i.e., the statistics of the number of eigenvalues in a given interval [12–16]. These observables can be computed exactly for the log-gas, thanks to certain special analytical structure of the particular form of the JPDF [1, 2]. Moreover, they have been measured experimentally in a variety of systems, from nuclear physics and quantum chaos [17] to liquid crystals [18] and fiber lasers [19]. Unfortunately, there exist very few long-ranged interacting gases, even in one-dimension, for which these observables can be computed, with perhaps the exception of the $1d$ -jellium model [20–

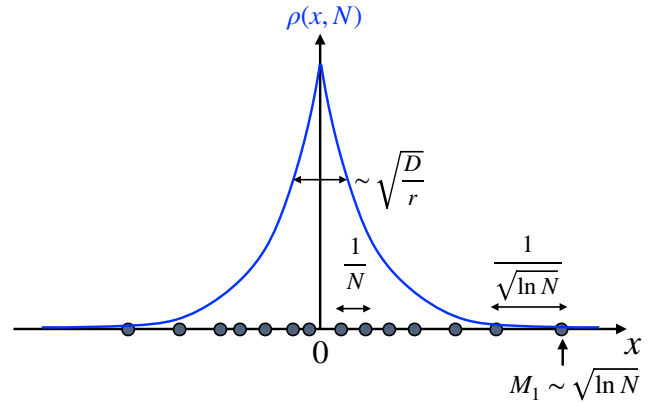


FIG. 1. The solid blue line shows the average density $\rho(x, N) = \sqrt{\frac{r}{4D}} e^{-\sqrt{r/D}|x|}$. The positions of the particles in a typical sample are shown schematically on the line with most particles living over a distance $\sqrt{D/r}$ around the origin. The typical spacing in the bulk $\sim 1/N$, while it is of order $\sim 1/\sqrt{\ln N}$ near the extreme edges of the sample. The typical position of the rightmost particle $M_1 \sim \sqrt{\ln N}$ for large N .

26]. It is therefore natural to look for other experimentally realisable long-ranged interacting particle systems for which these observables can be computed analytically. Motivated by the recent theoretical and experimental advances in the field of stochastic resetting [27–29], in this Letter we propose a new model of interacting particles that is simple yet solvable for all these observables, despite the presence of strong correlations.

A single particle subjected to stochastic resetting has been studied extensively over the last decade [30–46]. Consider, for simplicity, a single Brownian particle diffusing on a line with diffusion constant D , starting at the origin. With rate r , the particle's position is reset back to the origin and the free diffusion restarts. This resetting move breaks detailed balance and drives the system into a non-equilibrium stationary state (NESS) where the

position distribution becomes non-Gaussian [30, 31]

$$P_{\text{stat}}(x) = \frac{1}{2} \sqrt{\frac{r}{D}} e^{-|x|\sqrt{\frac{r}{D}}}. \quad (1)$$

This simple analytical prediction has been verified in recent experiments using holographic optical tweezers [43]. In this Letter, we consider N independent Brownian particles on a line, all starting at the origin, that are *simultaneously* reset to the origin with rate r (this is different from independently reset Brownian particles studied before [30, 47]). This *simultaneous* resetting makes the system strongly correlated, and this correlation persists even in the resulting many-body NESS at long times. To compute this steady state, we use a renewal approach. First, we note that without resetting, the JPDF of the positions at time t has a factorised form due to the independence of the Brownian particles $P_0[\{x_i\}, t] = \prod_{i=1}^N \frac{1}{\sqrt{4\pi Dt}} e^{-\frac{x_i^2}{4Dt}}$. In the presence of resetting with constant rate r the JPDF reads

$$P_r[\{x_i\}, t] = e^{-rt} P_0[\{x_i\}, t] + r \int_0^t d\tau e^{-r\tau} P_0[\{x_i\}, \tau] \quad (2)$$

This can be understood easily by considering the number of resetting events in the time interval $[0, t]$. If there is no resetting, which occurs with probability e^{-rt} , the JPDF is just $P_0[\{x_i\}, t]$. This explains the first term in (2). The second term arises from events with more than one resetting in $[0, t]$. In this case, the position distribution of the particles depends only on the time elapsed since the last resetting to the origin. Let $t - \tau$ denote the instant at which the last resetting before t takes place. The probability that this last interval $[t - \tau, t]$ of length τ is reset-free is $e^{-r\tau}$, while the probability of having a resetting event preceding this interval is $r d\tau$. During this last reset-free interval, the system has a free propagation starting at the origin. Since this is a Markov process, it does not remember the previous history and the position distribution only depends on the time since the last resetting, explaining the factor $P_0[\{x_i\}, \tau]$ in the second term. In the long-time limit, the first term in (2) drops out and we obtain the exact JPDF in the stationary state

$$P_{\text{stat}}[\{x_i\}] = r \int_0^\infty d\tau e^{-r\tau} \prod_{i=1}^N \frac{1}{\sqrt{4\pi D\tau}} e^{-\frac{x_i^2}{4D\tau}}. \quad (3)$$

Thus one sees that, while the integrand has a factorisable form, the integral over τ makes the particle positions correlated. This integral can, in fact, be performed explicitly

$$P_{\text{stat}}[\{x_i\}] = \left(\frac{r}{2\pi D}\right)^{\frac{N}{2}} R_N^{\frac{2-N}{2}} K_{\frac{N}{2}-1}(R_N), \quad (4)$$

where $R_N = \sqrt{\frac{r}{D}} \sqrt{x_1^2 + \dots + x_N^2}$ and $K_\nu(z)$ is the modified Bessel function of index ν . This makes the correlated nature of the gas manifest, though unlike the

log-gas the correlation is not pairwise but rather ‘‘all-to-all’’. Let us remark that one can interpret this stationary state as that of a single resetting Brownian particle in N dimensions [32]. However, here we need to interpret x_1, x_2, \dots, x_N as the positions of N particles on a line, rather than the components of an N -dimensional vector, since observables like the spacing distribution or the FCS make sense only in the former interpretation. Finally, to see that this resetting gas indeed has long range correlations, we compute the two-point correlations from the JPDF in Eq. (3). Noting that $\langle x_i x_j \rangle - \langle x_i \rangle \langle x_j \rangle = 0$ (for $i \neq j$) trivially, the first non-trivial correlator is given by

$$\langle x_i^2 x_j^2 \rangle - \langle x_i^2 \rangle \langle x_j^2 \rangle = \frac{4D^2}{r^2} \quad \forall i, j, \quad (5)$$

which manifestly demonstrates the long-range correlations.

Given the JPDF in Eq. (3), our goal is to compute the four basic and natural observables mentioned in the introduction. The reason why these observables can be computed exactly can be seen in the structure of the JPDF in Eq. (3), where the integrand (modulo $e^{-r\tau}$) just corresponds to a set of N independent and Gaussian distributed random variables, parametrised by τ . For a fixed τ , we first compute the statistics of these observables for N independent and identically distributed (IID) Gaussian random variables and then integrate over τ . We will see that just this simple mechanism leads to the rather rich and interesting behaviors of these observables.

We start with the first basic observable, namely the average density of particles in the stationary state, defined by $\rho(x, N) = \frac{1}{N} \langle \sum_{i=1}^N \delta(x - x_i) \rangle$, where $\langle \dots \rangle$ denotes the average over the stationary measure in (3). Thus $\rho(x, N)$, normalised to unity, measures the average fraction of particles in $[x, x + dx]$. Using the invariance of the JPDF in (3) under exchange of i and j , one sees that $\rho(x, N)$ is also the one-point function $\rho(x, N) = \int_{-\infty}^\infty dx_2 \dots dx_N P_r(x, x_2, \dots, x_N)$. Using the factorisation property in Eq. (3), one sees that $\rho(x, N)$ coincides with the position distribution $P_{\text{stat}}(x)$ of a single particle given in Eq. (1) and plotted in Fig. 1. Thus, $\rho(x, N)$ is independent of N and is supported over the full line (as opposed to the celebrated Wigner semi-circular law in RMT, where the density of eigenvalues depends on N and has a finite support for large N [6]).

Moreover, from Eq. (1), one sees that the density decreases exponentially over a length scale $\sqrt{D/r}$ where most particles are concentrated in a typical sample (see Fig. 1). Hence the typical spacing between particles in the bulk scales as $\sim O(1/N)$ for large N . While the average density extends over the full space, in a typical sample, the rightmost (or leftmost) particle is located at a distance of order $O(\sqrt{\ln N})$ from the center (see later). In addition, the spacing between two particles near these extremes scales as $1/\sqrt{\ln N} \gg 1/N$. Thus in a typical

sample the gas is more dense near the center and sparse near the extremes, as illustrated in Fig. 1.

Having computed the global density, we now probe the gas at a local level by studying the statistics of the positions of individual particles and the spacing between them. For this, it is convenient to first order the positions $\{x_1, x_2, \dots, x_N\}$ and label them as $\{M_1 > M_2 > \dots > M_N\}$ where M_k denotes the position of the k -th particle counted from the right. Thus $M_1 = \max\{x_1, x_2, \dots, x_N\}$ denotes the global maximum, i.e., the position of the rightmost particle. Using Eq. (3), the cumulative distribution of M_1 is clearly given by

$$\text{Prob.}(M_1 \leq w) = r \int_0^\infty d\tau e^{-r\tau} \text{Prob.}[M_1(\tau) \leq w] \quad (6)$$

where $M_1(\tau)$ denotes the maximum of N IID Gaussian random variables, parametrised by τ . The distribution of the maximum of N IID random variables is well known from the theory of extreme value statistics (EVS) [48–51]. One finds that, to leading order for large N , the random variable $M_1(\tau)$ converges to

$$M_1(\tau) \approx a_N(\tau) + b_N(\tau) z_1 \quad , \quad \text{where} \\ a_N(\tau) = \sqrt{4D\tau \ln\left(\frac{N}{2}\right)} \quad , \quad b_N(\tau) = \sqrt{\frac{D\tau}{\ln\left(\frac{N}{2}\right)}} \quad , \quad (7)$$

and z_1 is a random variable (of order $O(1)$) distributed via the Gumbel law, i.e., $\text{Prob.}(z_1 \leq w) = e^{-e^{-w}}$. Inserting this result for $M_1(\tau)$ in Eq. (6), it turns out that the fluctuations of $M_1(\tau)$ of order $O(1/\sqrt{\ln N})$ in (7) do not contribute to this integral over τ to leading order (see Supplementary Material). Thus, very conveniently, one can approximate for large N , $\text{Prob.}(M_1(\tau) \leq w) = \theta(w - a_N(\tau))$ where $\theta(z)$ is the Heaviside step function. Substituting this in Eq. (6) and performing the integral trivially, we get $\text{Prob.}(M_1 \leq w) \approx 1 - e^{-\frac{w^2}{L_N^2}}$ where the scale $L_N = \sqrt{4D \ln(N/2)/r}$ increases extremely slowly with N . The probability distribution function (PDF) of M_1 can then be obtained by differentiation and takes the scaling form

$$P(M_1) \approx \frac{1}{L_N} f\left(\frac{M_1}{L_N}\right) \quad , \quad f(z) = 2z e^{-z^2} \quad , \quad (8)$$

for $z \geq 0$. Thus, even though the global density extends over the full space and is independent of N [see Eq. (1)], the maximum in a given sample scales as $\sqrt{\ln N}$ for large N . Moreover, the scaled distribution $f(z)$ in (8) is very different from the Gumbel distribution of uncorrelated variables, demonstrating that strong correlations do affect drastically the EVS. The extreme value distribution in this resetting gas is the analogue of the Tracy-Widom distribution for the position of the rightmost particle in the Dyson's log-gas [8–11].

The computation for M_1 can be easily extended to M_k , both when $k = O(1)$ (near the extremes of the gas) as

well as $k = \alpha N$, with $0 \leq \alpha \leq 1$, corresponding to the position of a particle in the bulk [52]. Interestingly, we find that the appropriately scaled distribution of M_k is independent of k and is given by the same universal scaling function (8). This result is confirmed in our numerical simulations as shown in Fig. 2 a).

We now turn to the distribution of the spacing (or gap) between two consecutive particles $d_k = M_k - M_{k+1}$. We first consider $k = O(1)$, corresponding to the spacing between particles near the maximum M_1 . Starting from the JPDF in Eq. (3) we first calculate the distribution of the gap $d_k(\tau) = M_k(\tau) - M_{k+1}(\tau)$ where $M_k(\tau)$ denotes the k -th maximum of N IID Gaussian random variables parametrised by τ . As in the case of $k = 1$ [see Eq. (7)], it is known from the theory of EVS of IID variables, that the random variable $M_k(\tau)$ converges for large N to [49–51]

$$M_k(\tau) \approx a_N(\tau) + b_N(\tau) z_k \quad , \quad (9)$$

where $a_N(\tau)$ and $b_N(\tau)$ are the same as in Eq. (7), but z_k is distributed via the generalized Gumbel distribution $\text{Prob.}(z_k = w) = \frac{1}{(k-1)!} e^{-kw - e^{-w}}$. Since the leading deterministic term $a_N(\tau)$ in Eq. (9) is independent of k , the gap $d_k(\tau) = M_k(\tau) - M_{k+1}(\tau)$ is sensitive to fluctuations of $M_k(\tau)$ and is given by $d_k(\tau) = b_N(\tau)(z_k - z_{k+1}) = b_N(\tau) s_k$. The variable $s_k \geq 0$ is known to be exponentially distributed as $\text{Prob.}(s_k = s) = k e^{-k s}$ [49–51]. Therefore, the spacing distribution in the resetting gas near the extremes can be written as

$$P(d_k) = r \int_0^\infty d\tau e^{-r\tau} \text{Prob.}(b_N(\tau) s_k = d_k) \quad . \quad (10)$$

Substituting the exponential distribution for s_k , one can express this gap PDF in the scaling form

$$P(d_k) \approx \frac{1}{\ell_N(k)} h\left(\frac{d_k}{\ell_N(k)}\right) \quad , \quad h(z) = 2 \int_0^\infty du e^{-u^2 - \frac{z}{u}} \quad (11)$$

where the scale $\ell_N(k) = \sqrt{\frac{D}{r k^2 \ln(N/2)}}$. The scaling function $h(z) \rightarrow \sqrt{\pi}$ as $z \rightarrow 0$, has a stretched exponential tail $h(z) \sim e^{-3(z/2)^{2/3}}$ for large z (see [52]), and is normalised to unity $\int_0^\infty h(z) dz = 1$. Numerical simulations are in excellent agreement with this prediction [see Fig. 2 b)]. The stretched exponential tail of the gap scaling function is a clear signature of strong correlations in the gas. Note that in the IID Gaussian case, the gap distribution is purely exponential [50].

What about the spacing distribution in the bulk, when $k = \alpha N$ with fixed $0 < \alpha < 1$? In this case, one can again show that for the IID Gaussian variables parametrised by τ , the gap $d_k(\tau)$ converges to (see Supplementary Material)

$$d_k(\tau) = M_k(\tau) - M_{k+1}(\tau) \approx \frac{s}{Np(y_0, \tau)} \quad (12)$$

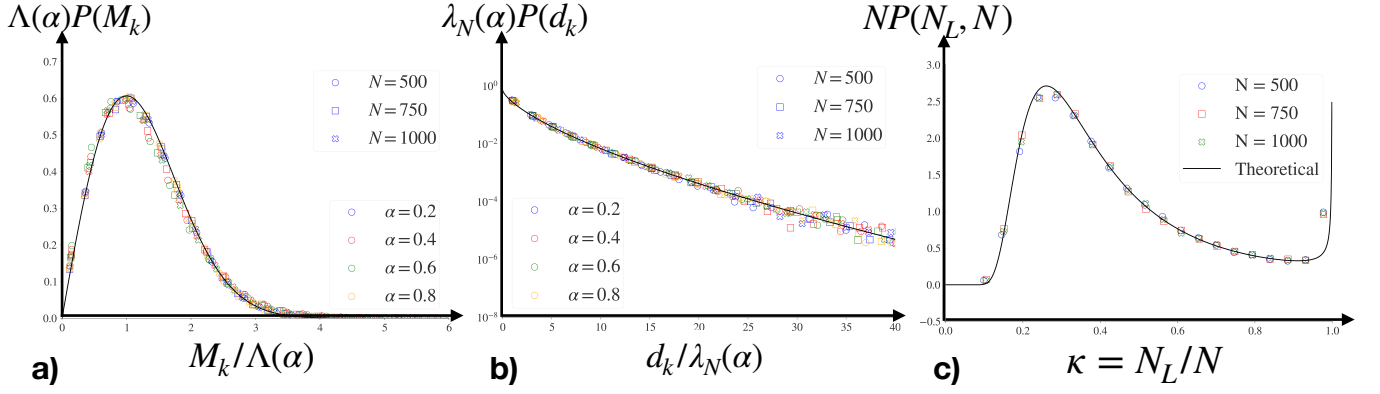


FIG. 2. **a)** Scaled distribution of the k -th particle from the right: $P(M_k) \approx \Lambda^{-1}(\alpha)f(M_k\Lambda^{-1}(\alpha))$ with $\Lambda(\alpha)$ given in Eq. (19) of Supp. Mat. [52]. The symbols represent the results of simulations, while the solid curve shows the scaling function $f(z)$ in Eq. (8). **b)** Scaled distribution of the gap $d_k = M_k - M_{k+1}$ between the k -th and the $(k+1)$ -th particle counted from the right: numerical simulations are in perfect agreement with the analytical scaling function $h(z)$ in Eq. (14). **c)** Numerical results for FCS in $[-L, +L]$ (with $L = 0.4$) compared with the analytical predictions in Eqs. (17) and (18). We used the parameter values $D = 0.5$ and $r = 1$.

where $s \geq 0$ has a purely exponential distribution $P(s) = e^{-s}$, independently of k . In Eq. (12), $p(y, \tau) = e^{-y^2/(4D\tau)}/\sqrt{4\pi D\tau}$ and y_0 is determined from the quantile relation $\int_{y_0}^{\infty} p(y, \tau) dy = \alpha$ which fixes the fraction of particles to the right of y_0 to be α . Indeed, for this Gaussian $p(y, \tau)$, one can write explicitly $y_0 = B\sqrt{4D\tau}$ with $B = \text{erfc}^{-1}(2\alpha)$ where $\text{erfc}(z) = \frac{2}{\sqrt{\pi}} \int_z^{\infty} e^{-u^2} du$ and $\text{erfc}^{-1}(z)$ denotes its inverse function. Consequently $p(y_0, \tau) = \exp(-B^2)/\sqrt{4\pi D\tau}$. Hence the analogue of Eq. (10) in the bulk reads

$$P(d_k) = r \int_0^{\infty} d\tau e^{-r\tau} \text{Prob.} \left(\frac{s}{Np(y_0, \tau)} = d_k \right) \quad (13)$$

Using the exponential distribution of s , one can then write the gap distribution in the scaling form

$$P(d_k) \approx \frac{1}{\lambda_N(\alpha)} h \left(\frac{d_k}{\lambda_N(\alpha)} \right), \quad (14)$$

where $h(z)$ is exactly the same scaling function as in (11) valid for gaps near the extremes, but the scale factor $\lambda_N(\alpha) = \sqrt{\frac{4\pi D}{r}} e^{B^2} \frac{1}{N}$ is quite different from $\ell_N(k)$. Note that the α -dependence is encoded in the constant $B = \text{erfc}^{-1}(2\alpha)$. Thus, quite surprisingly, the scaling functions for the spacing distribution are the same both in the bulk and near the extremes. This is very different from the log-gas case where the bulk [1, 2] and the edge [53] gaps behave quite differently.

Finally, we turn to the FCS, i.e., the distribution $P(N_L, N)$ of the number of particles N_L contained in a symmetric interval $[-L, +L]$ around the resetting position which is $x = 0$ here. It reads

$$P(N_L, N) = r \int_0^{\infty} d\tau e^{-r\tau} \binom{N}{N_L} [q(\tau)]^{N_L} [1 - q(\tau)]^{N - N_L} \quad (15)$$

Here $q(\tau) = \int_{-L}^L p(y, \tau) dy = \text{erf}(L/\sqrt{4D\tau})$ with $\text{erf}(z) = 1 - \text{erfc}(z)$ which denotes the probability that a single Brownian particle, at time τ , is inside the interval $[-L, +L]$. The binomial distribution inside the integrand just denotes the probability that N_L , out of N independent particles, are in the interval $[-L, +L]$ at time τ . Setting $N_L = \kappa N$, with $0 < \kappa < 1$ fixed, the binomial distribution converges to a Gaussian distribution with mean $Nq(\tau)$ and variance $Nq(\tau)(1 - q(\tau))$. As in the case of the maximum M_1 , the fluctuations of this Gaussian variable do not contribute to the integral in the large N limit and one can replace the Gaussian by a delta-function $\delta(N_L - Nq(\tau))$ leading to

$$P(N_L, N) \approx \frac{r}{N} \int_0^{\infty} d\tau e^{-r\tau} \delta(\kappa - q(\tau)). \quad (16)$$

Using the explicit form of $q(\tau)$, the integral over τ can now be performed by a change of variable and $P(N_L, N)$ takes the scaling form

$$P(N_L, N) \approx \frac{1}{N} H(\kappa), \quad (17)$$

where $\kappa = \frac{N_L}{N}$ and the scaling function $H(\kappa)$ is given by

$$H(\kappa) = \gamma\sqrt{\pi} [u(\kappa)]^{-3} \exp \left[-\frac{\gamma}{u(\kappa)^2} + [u(\kappa)]^2 \right] \quad (18)$$

where $\gamma = rL^2/(4D)$ and $u(\kappa) = \text{erf}^{-1}(\kappa)$. The PDF $H(\kappa)$ of $0 \leq \kappa \leq 1$ is normalised to unity $\int_0^1 H(\kappa) d\kappa = 1$ and has an unusual non-trivial shape [see Fig. 2 c)]. As $\kappa \rightarrow 0$, the function $H(\kappa) \approx \frac{8\gamma}{\pi\kappa^3} \exp(-\frac{4\gamma}{\pi\kappa^2})$ vanishes very fast, while it diverges (though still integrable) as $H(\kappa) \approx \frac{\gamma\sqrt{\pi}}{(1-\kappa)|\ln(1-\kappa)|^{3/2}}$ as $\kappa \rightarrow 1$. Numerical simulations are in very good agreement with our analytical prediction in Eq. (18). Thus the scaling form of FCS in

Eqs. (17)-(18) is fundamentally different from the log-gas case. Here the mean and standard deviation of N_L both scale as N , while in the log-gas the mean scales as N and the Gaussian fluctuations around the mean have standard deviation $\sim \sqrt{\ln N}$ [12–16].

To summarise, we have presented the exact solution of a resetting gas with long range correlations in the steady state and computed several observables of interest. Apart from the celebrated log-gas, this is one of the few solvable models with strong correlations. In addition, this resetting gas is also experimentally realisable. A single diffusing particle with resetting has been recently realised in optical trap experiments [44, 45], where the particle is allowed to diffuse freely for a random time after which a trap is switched on. The particle is relaxed to its equilibrium in the trap using the "engineering swift equilibration" (ESE) technique [54]. This mimics the resetting move of the particle to its equilibrium distribution. The same protocol, via ESE, can then be easily implemented to simultaneously reset many noninteracting particles in the same optical trap. We thus hope that our analytical predictions will stimulate further experimental studies of such a resetting gas.

-
- [1] M. L. Mehta, *Random matrices*, Elsevier (2004)
- [2] P. J. Forrester, *Log-Gases and Random Matrices*, (London Mathematical Society monographs, 2010)
- [3] G. Livan, M. Novaes, P. Vivo, *Introduction to random matrices theory and practice*, Monograph Award, 63 (2018)
- [4] M. Potters, J. P. Bouchaud, *A First Course in Random Matrix Theory: For Physicists, Engineers and Data Scientists*, Cambridge University Press (2020)
- [5] F. J. Dyson, *J. Math. Phys.* **3**, 140 (1962)
- [6] E. P. Wigner, *Ann. Math.* **67**, 325 (1958)
- [7] E. P. Wigner, *Math. Proc. Cambridge Philos. Soc.* **47**, 790 (1951)
- [8] C. A. Tracy, H. Widom, *Commun. Math. Phys.* **159**, 151 (1994)
- [9] C. A. Tracy, H. Widom, *Commun. Math. Phys.* **177**, 727 (1996)
- [10] J. Baik, P. Deift, K. Johansson, *J. Amer. Math. Soc.* **12**, 1119 (1999)
- [11] S. N. Majumdar, G. Schehr, *J. Stat. Mech.*, 01012 (2014)
- [12] M. M. Fogler, B. I. Shklovskii, *Phys. Rev. Lett.* **74**, 3312 (1995)
- [13] O. Costin, J. L. Lebowitz, *Phys. Rev. Lett.* **75**, 69 (1995)
- [14] S. N. Majumdar, C. Nadal, A. Scardicchio, P. Vivo, *Phys. Rev. Lett.* **103**, 220603 (2009)
- [15] R. Marino, S. N. Majumdar, G. Schehr, P. Vivo, *Phys. Rev. Lett.* **112**, 254101 (2014)
- [16] N. R. Smith, P. Le Doussal, S. N. Majumdar, G. Schehr, *SciPost Phys.* **11**, 110 (2021)
- [17] H. A. Weidenmüller, G. E. Mitchell, *Rev. Mod. Phys.* **81**, 539 (2009)
- [18] K. A. Takeuchi, M. Sano, *Phys. Rev. Lett.* **104**, 230601 (2010)
- [19] M. Fridman, R. Pugatch N. Nixon, A. A. Friesem, N. Davidson, *Phys. Rev. E* **85** R020101(2012)
- [20] A. Lenard, *J. Math. Phys.* **2** 682 (1961)
- [21] S. Prager, *Adv. Chem. Phys.* **4**, 201 (1962)
- [22] R. J. Baxter, *Math. Proc. Camb. Phil. Soc.* **59**, 779 (1963)
- [23] A. Dhar, A. Kundu, S. N. Majumdar, S. Sabhapandit, G. Schehr, *Phys. Rev. Lett.* **119**, 060601 (2017)
- [24] A. Dhar, A. Kundu, S. N. Majumdar, S. Sabhapandit, G. Schehr, *J. Phys. A: Math. Theor.* **51**, 295001 (2018)
- [25] D. Chafaï, D., García-Zelada, P. Jung, *Bernoulli* **28**, 1784 (2022)
- [26] A. Flack, S. N. Majumdar, G. Schehr, *J. Stat. Mech.*, 053211 (2022)
- [27] M. R. Evans, S. N. Majumdar, and G. Schehr, *J. Phys. A* **53**, 193001 (2020)
- [28] A. Pal, S. Kostinski, S. Reuveni, *J. Phys. A: Math. Theor.* **55**, 021001 (2022)
- [29] S. Gupta, A. M. Jayannavar, *Frontiers in Physics* **10**, 789097 (2022)
- [30] M. R. Evans, S. N. Majumdar, *Phys. Rev. Lett.* **106**, 160601 (2011)
- [31] M. R. Evans, S. N. Majumdar, *J. Phys. A: Math. Theor.* **44**, 435001 (2011)
- [32] M. R. Evans, S. N. Majumdar, *J. Phys. A: Math. Theor.* **47**, 285001 (2014)
- [33] L. Kusmierz, S. N. Majumdar, S. Sabhapandit, G. Schehr, *Phys. Rev. Lett.* **113**, 220602 (2014)
- [34] S. N. Majumdar, S. Sabhapandit, G. Schehr, *Phys. Rev. E* **91**, 052131 (2015)
- [35] A. Pal, A. Kundu, and M. R. Evans, *J. Phys. A: Math. Theor.* **49**, 225001 (2016)
- [36] S. Reuveni, *Phys. Rev. Lett.* **116**, 170601 (2016)
- [37] M. Montero, J. Villarroel, *Phys. Rev. E* **94**, 032132 (2016)
- [38] A. Pal, S. Reuveni, *Phys. Rev. Lett.* **118**, 030603 (2017)
- [39] D. Boyer, M. R. Evans, S. N. Majumdar, *J. Stat. Mech.*, 023208 (2017)
- [40] A. Chechkin, I. M. Sokolov, *Phys. Rev. Lett.* **121**, 050601 (2018)
- [41] P. C. Bressloff, *J. Phys. A: Math. Theor.* **53**, 425001 (2020)
- [42] R. G. Pinsky, *Stoch. Proc. Appl.* **130**, 2954 (2020)
- [43] O. Tal-Friedman, A. Pal, A. Sekhon, S. Reuveni, Y. Roichman, *J. Phys. Chem. Lett.* **11**, 7350 (2020)
- [44] B. Besga, A. Bovon, A. Petrosyan, S. N. Majumdar, S. Ciliberto, *Phys. Rev. Research* **2**, 032029(R) (2020)
- [45] F. Faisant, B. Besga, A. Petrosyan, S. Ciliberto, S. N. Majumdar, *J. Stat. Mech.*, 113203 (2021)
- [46] B. De Bruyne, S. N. Majumdar, G. Schehr, *Phys. Rev. Lett.* **128**, 200603 (2022)
- [47] O. Vilck, M. Assaf, B. Meerson, *Phys. Rev. E* **106**, 024117 (2022)
- [48] E. J. Gumbel, *Statistics of Extremes* (Dover, New York, 1958)
- [49] H. A. David, H. N. Nagaraja, *Order statistics*, John Wiley & Sons (2004).
- [50] G. Schehr, S. N. Majumdar, In *First-passage phenomena and their applications*, Eds. R. Metzler, G. Oshanin, and S. Redner, (pp. 226-251), (World Scientific, Singapore, 2014), arXiv:1305.0639
- [51] S. N. Majumdar, A. Pal, G. Schehr, *Phys. Rep.* **840**, 1 (2020)

[52] See Supplementary Material

[53] A. Perret, G. Schehr, *J. Stat. Phys.* **156**, 843 (2014).

[54] I. A. Martinez, A. Petrosyan, D. Guéry-Odelin, E. Trizac, S. Ciliberto, *Nat. Phys.* **12**, 843 (2016)

Exact order, gap and counting statistics of a Brownian gas correlated by resetting: Supplemental material

Marco Biroli,¹ Hernan Larralde,² Satya N. Majumdar,¹ and Grégory Schehr³

¹*LPTMS, CNRS, Univ. Paris-Sud, Université Paris-Saclay, 91405 Orsay, France*

²*Instituto de Ciencias Fisicas, UNAM, Av. Universidad s/n, CP 62210 Cuernavaca Morelos, Mexico*

³*Sorbonne Université, Laboratoire de Physique Théorique et Hautes Energies,
CNRS UMR 7589, 4 Place Jussieu, 75252 Paris Cedex 05, France*

We give the principal details of the calculations described in the main text of the Letter.

I. DISTRIBUTION OF THE k -TH MAXIMUM

We consider the resetting gas in the steady state with positions $\{x_1, x_2, \dots, x_N\}$ ordered as $\{M_1 > M_2 > \dots > M_N\}$, where M_k denotes the position of the k -th maximum, i.e., the position of the k -th particle counted from the right. The probability distribution function (PDF) of M_k is

$$\text{Prob.}(M_k = w) = r \int_0^\infty d\tau e^{-r\tau} \text{Prob.}(M_k(\tau) = w), \quad (1)$$

where $M_k(\tau)$ is the k -th maximum of a set of N independent and identically distributed (IID) random variables, each drawn from the Gaussian distribution parametrised by τ

$$p(y, \tau) = \frac{1}{\sqrt{4\pi D\tau}} e^{-\frac{y^2}{4D\tau}}. \quad (2)$$

We now consider the limiting distribution of M_k for large N in two separate cases: (i) when $k = O(1)$, i.e., distribution of the k -th maximum close to the global maximum and (ii) when $k = \alpha N$ with $\alpha = O(1)$, which provides the distribution of the ordered maximum in the bulk, i.e., near the origin.

A. k -th maximum for $k = O(1)$

It is well known from the EVS of IID random variables that in the large N limit, the PDF of $M_k(\tau)$, for fixed $k = O(1)$, converges to the following distribution [1–3]

$$\text{Prob.}(M_k(\tau) = w) \rightarrow \frac{1}{b_N(\tau)} G_k \left(\frac{w - a_N(\tau)}{b_N(\tau)} \right), \quad (3)$$

where

$$a_N(\tau) \approx \sqrt{4D\tau \ln(N/2)} \quad , \quad b_N(\tau) \approx \sqrt{\frac{D\tau}{\ln(N/2)}} \quad (4)$$

$$(5)$$

and $G_k(z)$ is the generalized Gumbel PDF

$$G_k(z) = \frac{1}{(k-1)!} e^{-kz - e^{-z}}. \quad (6)$$

We now insert this scaling form (3) in the integral in Eq. (1) and perform the change of variable $\tau \rightarrow z$ with

$$\frac{w - a_N(\tau)}{b_N(\tau)} = z \quad \implies \quad \tau = \frac{\ln(N/2)}{D} \frac{w^2}{(z + 2 \ln(N/2))^2}. \quad (7)$$

Taking the scaling limit $N \rightarrow \infty$, $w \rightarrow \infty$ but keeping $w/\sqrt{\ln(N/2)}$ fixed and using the normalization $\int_{-\infty}^\infty G_k(z) dz = 1$, one gets from Eq. (1)

$$\text{Prob.}(M_k = w) \approx \frac{r w}{2D \ln(N/2)} \exp \left(-\frac{r w^2}{4D \ln(N/2)} \right). \quad (8)$$

Then the PDF $P(M_k)$ of the k -th maximum can be written in the scaling form

$$P(M_k) \approx \frac{1}{L_N} f \left(\frac{M_k}{L_N} \right) \quad \text{with} \quad L_N = \sqrt{\frac{4D \ln(N/2)}{r}} \quad (9)$$

and the scaling function $f(z)$ is given by

$$f(z) = 2ze^{-z^2} \quad , \quad z \geq 0. \quad (10)$$

Thus, both the scale factor L_N as well as the scaling function $f(z)$ are independent of the index k of the maximum, as long as $k = O(1)$ when $N \rightarrow \infty$. In particular, putting $k = 1$ gives the distribution of the global maximum M_1 , as stated in Eq. (8) of the main text.

Note that this leading large N result in Eq. (10) is equivalent to replacing the scaling form in Eq. (3) by a δ -function, i.e.,

$$\text{Prob.}(M_k(\tau) = w) \approx \delta(w - a_N(\tau)) . \quad (11)$$

In other words, the fluctuations of $M_k(\tau)$ do not contribute to the distribution of M_k , to leading order for large N , as discussed in the main text after Eq. (7).

B. k -th maximum for $k = \alpha N$

The starting point is again the expression given in Eq. (1). We need to find the distribution of the k -th maximum of a set of N IID Gaussian random variables, each distributed via $p(y, \tau)$ in Eq. (2), which is parametrised by τ . We will now work in the bulk limit, i.e., we first set $k = \alpha N$ and take the large N limit, keeping α fixed. Let us first work out the limiting distribution of the k -th maximum $M_k(\tau)$ for fixed τ and $k = \alpha N$. The PDF of the k -th maximum of N IID random variables is given by the well known formula

$$\text{Prob.}(M_k(\tau) = w) = \frac{N!}{(k-1)!(N-k)!} p(w, \tau) \left[\int_w^\infty p(y, \tau) dy \right]^{k-1} \left[\int_{-\infty}^w p(y, \tau) dy \right]^{N-k} . \quad (12)$$

This formula can be understood as follows. Out of N IID variables, we fix the value of the k -th maximum to be w , then there are $(k-1)$ variables above w and $(N-k)$ variables below w . Using the independence of the variables and taking into account the number of ways of arranging this ordering (this is encoded in the combinatorial factor in Eq. (12)), one arrives at Eq. (12). We now set $k = \alpha N$ and rewrite this as

$$\text{Prob.}(M_k(\tau) = w) = \frac{N!}{\Gamma(\alpha N) \Gamma[(1-\alpha)N + 1]} \frac{p(w, \tau)}{\int_w^\infty p(y, \tau) dy} e^{-N\Phi_\alpha(w)} \quad (13)$$

where

$$\Phi_\alpha(w) = -\alpha \ln \left(\int_w^\infty p(y, \tau) dy \right) - (1-\alpha) \ln \left(\int_{-\infty}^w p(y, \tau) dy \right) . \quad (14)$$

Note that, for convenience, we have expressed the factorials in terms of Gamma functions in Eq. (13). This formula (13) is exact for all N . As $N \rightarrow \infty$, this PDF gets sharply peaked around the minimum of $\Phi_\alpha(w)$, say at w^* . The location of this minimum w^* can be easily computed by minimising $\Phi_\alpha(w)$. Setting $\Phi'_\alpha(w = w^*) = 0$ one immediately gets

$$\int_{w^*}^\infty p(y, \tau) dy = \alpha . \quad (15)$$

Note that w^* is called the α -quantile as it denotes the location of y above which the average fraction of particles is α .

In our case $p(y, \tau)$ is a Gaussian distribution given in (2) and this relation (15) reads explicitly

$$w^* = \sqrt{4D\tau} \operatorname{erfc}^{-1}(2\alpha) , \quad (16)$$

where $\operatorname{erfc}(z) = \frac{2}{\sqrt{\pi}} \int_z^\infty e^{-u^2} du$ is the complementary error function and $\operatorname{erfc}^{-1}(z)$ is its inverse. Expanding $\Phi_\alpha(w)$ around $w = w^*$ up to quadratic order, one finds after straightforward algebra that around $w = w^*$, and for large N , the PDF of $M_k(\tau)$ takes a Gaussian form

$$\text{Prob.}(M_k(\tau) = w) \approx \sqrt{\frac{N}{2\pi\alpha(1-\alpha)}} p(w^*, \tau) \exp \left(-\frac{N p^2(w^*, \tau)}{2\alpha(1-\alpha)} (w - w^*)^2 \right) . \quad (17)$$

This is a normalised Gaussian distribution centered around w^* and with a width that decays as $1/\sqrt{N}$ for large N . Indeed, for large N , it essentially approaches a delta-function, centered at $w = w^*$ given in Eq. (16).

Now we substitute this limiting Gaussian distribution in Eq. (1). As discussed before, it turns out that the fluctuations of $M_k(\tau)$ around its mean w^* do not contribute to leading order for large N . One can then replace in the integrand in Eq. (1)

$$\text{Prob.}(M_k(\tau) = w) \approx \delta(w - w^*) = \delta \left(w - \sqrt{4D\tau} \operatorname{erfc}^{-1}(2\alpha) \right) . \quad (18)$$

Performing the resulting integral over τ trivially, we get for the PDF of M_k

$$P(M_k) \approx \frac{1}{\Lambda(\alpha)} f\left(\frac{M_k}{\Lambda(\alpha)}\right) \quad \text{with} \quad \Lambda(\alpha) = \sqrt{\frac{4D}{r}} \operatorname{erfc}^{-1}(2\alpha), \quad (19)$$

where $f(z) = 2z e^{-z^2}$ is the same scaling function as in the case $k = O(1)$ [see Eq. (10)]. Comparing Eqs. (19) and (9), we see that while the scale factors $\Lambda(\alpha)$ and L_N in the two cases are different, the scaling function $f(z)$ is completely universal, both in the bulk as well as near the global maximum. It is also easy to check that the distributions of M_k , for $k = O(1)$ and $k = O(N)$ match smoothly. This is easily seen by considering the scale factor $\Lambda(\alpha)$ when $\alpha = k/N \rightarrow 0$. In this case, using $\operatorname{erfc}^{-1}(2k/N) \approx \sqrt{\ln(N/2)}$ to leading order for large N (independently of k). Inserting this asymptotic behavior in $\Lambda(\alpha)$ as defined in (19), one sees that $\Lambda(\alpha) \rightarrow L_N$ as $\alpha = k/N \rightarrow 0$.

Summarizing the distribution of M_k for $k = O(1)$ and for $k = O(N)$, we obtain

$$P(M_k) \approx \begin{cases} \frac{1}{L_N} f\left(\frac{M_k}{L_N}\right) & \text{for } k = O(1) & \text{and } L_N = \sqrt{\frac{4D \ln(N/2)}{r}} \\ \frac{1}{\Lambda(\alpha)} f\left(\frac{M_k}{\Lambda(\alpha)}\right) & \text{for } k = O(N) & \text{and } \Lambda(\alpha) = \sqrt{\frac{4D}{r}} \operatorname{erfc}^{-1}(2\alpha), \end{cases} \quad (20)$$

where $f(z) = 2z e^{-z^2}$ ($z \geq 0$) is a universal scaling function, i.e., independent of k .

II. DISTRIBUTION OF THE k -TH GAP

By definition, the k -th gap is the distance between the positions of the k -th and the $(k+1)$ -th particle counted from the right, i.e., $d_k = M_k - M_{k+1}$. In the stationary state of the resetting gas, the distribution of the k -th gap is therefore given by

$$\operatorname{Prob.}(d_k = g) = r \int_0^\infty d\tau e^{-r\tau} \operatorname{Prob.}[M_k(\tau) - M_{k+1}(\tau) = g], \quad (21)$$

where $M_k(\tau)$, as before, is the k -th maximum of the N IID random variables, each distributed via the Gaussian distribution $p(y, \tau)$, parametrised by τ , in Eq. (2). Thus we need to first find the distribution of the gap $d_k(\tau) = M_k(\tau) - M_{k+1}(\tau)$ for fixed τ . For this we need to start with the joint distribution of $M_k(\tau)$ and $M_{k+1}(\tau)$ for N IID random variables

$$\operatorname{Prob.}[M_k(\tau) = x, M_{k+1}(\tau) = y] = \frac{N!}{(k-1)!(N-k-1)!} p(x, \tau) p(y, \tau) \left[\int_x^\infty p(x', \tau) dx' \right]^{k-1} \left[\int_{-\infty}^y p(x', \tau) dx' \right]^{N-k-1} \quad (22)$$

for $x > y$. The interpretation is again simple, as in Eq. (12). We choose two out of N variables and fix their positions at x and $y < x$. There are $(k-1)$ variables above x and $N-k-1$ variables below y . The combinatorial factor just counts the number of ways of ordering. As in the case of the k -th maximum, we consider the statistics of the k -th gap when $k = O(1)$ and $k = O(N)$ separately below.

A. k -th gap for $k = O(1)$

The case $k = O(1)$ has been studied extensively in the literature for IID random variables [2, 3] and one can show, starting from Eq. (22) that, in the limit $N \rightarrow \infty$ with k fixed,

$$d_k(\tau) \rightarrow b_N(\tau) s_k, \quad (23)$$

where $b_N(\tau) = \sqrt{D\tau/\ln(N/2)}$ and s_k is a random variable (independent of N) distributed via the exponential law

$$\operatorname{Prob.}(s_k = s) = k e^{-ks}, \quad s \geq 0. \quad (24)$$

As explained in the main text, by substituting the result (23) in (21), one arrives at the PDF of the k -th gap when $k = O(1)$

$$P(d_k) \approx \frac{1}{\ell_N(k)} h\left(\frac{d_k}{\ell_N(k)}\right) \quad \text{with} \quad \ell_N(k) = \sqrt{\frac{D}{r k^2 \ln(N/2)}}, \quad (25)$$

and the scaling function

$$h(z) = 2 \int_0^\infty du e^{-u^2 - \frac{z}{u}} , \quad (26)$$

as announced in Eq. (14) of the main text.

B. k -th gap for $k = O(N)$

We now set $k = \alpha N$ and rewrite Eq. (22) as

$$\text{Prob.}[M_k(\tau) = x, M_{k+1}(\tau) = y] = \frac{\Gamma(N+1)}{\Gamma(\alpha N)\Gamma[(1-\alpha)N]} U(x, \tau) V(y, \tau) e^{NS_\alpha(x, y)} , \quad (27)$$

where

$$U(x, \tau) = \frac{p(x, \tau)}{\int_x^\infty p(x', \tau) dx'} , \quad V(y, \tau) = \frac{p(y, \tau)}{\int_{-\infty}^y p(y', \tau) dy'} , \quad (28)$$

and $S_\alpha(x, y)$ reads

$$S_\alpha(x, y) = \alpha \ln \left[\int_x^\infty p(x', \tau) dx' \right] + (1-\alpha) \ln \left[\int_{-\infty}^y p(x', \tau) dx' \right] . \quad (29)$$

From this joint distribution (27) one can compute the gap distribution by setting $x = y + g$ and integrating over y with $g \geq 0$ fixed. This gives

$$\text{Prob.}(d_k(\tau) = g) = \frac{\Gamma(N+1)}{\Gamma(\alpha N)\Gamma[(1-\alpha)N]} \int_{-\infty}^\infty dy U(y+g, \tau) V(y, \tau) e^{NS_\alpha(y+g, y)} . \quad (30)$$

In the large N limit, this form suggests to evaluate the integral over y using a saddle point method. The saddle point is attained at $y = y^*$ where $\partial S / \partial y|_{y=y^*} = 0$. We expect that, in the bulk, the typical gap scales as $O(1/N)$ and hence is small. Therefore one can find the solution of the saddle point equation y^* in powers of g and one finds that

$$y^* = w^* + A g + O(g^2) \quad \text{with} \quad \int_{w^*}^\infty p(y, \tau) dy = \alpha . \quad (31)$$

where A is a computable constant, whose actual value turns out to be irrelevant to leading order in the large N limit. In our case w^* is given exactly in Eq. (16). Evaluating the saddle-point action at $y = y^*$ one gets,

$$S(y^* + g, y^*) = \alpha \ln \alpha + (1-\alpha) \ln(1-\alpha) - p(w^*, \tau) g + O(g^2) . \quad (32)$$

The first two terms in Eq. (32) cancel exactly the combinatorial factor in (30), expanded using Stirling's formula for large N . Evaluating this integral over y by the saddle point method and carefully collecting all the factors, we find, after a bit of algebra, a rather simple expression, namely

$$\text{Prob.}(d_k(\tau) = g) \approx N p(w^*, \tau) e^{-N p(w^*, \tau) g} \quad \text{where} \quad w^* = \sqrt{4D\tau} \text{erfc}^{-1}(2\alpha) \quad (33)$$

and $p(w^*, \tau)$ reads explicitly

$$p(w^*, \tau) = \frac{1}{\sqrt{4\pi D\tau}} \exp(-B^2) \quad \text{where} \quad B = \text{erfc}^{-1}(2\alpha) . \quad (34)$$

Finally, substituting this scaling form (33) in Eq. (21), one finds after a simple change of variable that the PDF of the k -th gap with $k = \alpha N$ can be expressed in the scaling form [see Eq. (14) in the main text]

$$P(d_k) \approx \frac{1}{\lambda_N(\alpha)} h\left(\frac{d_k}{\lambda_N(\alpha)}\right) \quad \text{with} \quad , \quad \lambda_N(\alpha) = \sqrt{\frac{4\pi D}{r}} \frac{e^{B^2}}{N} , \quad (35)$$

where we recall that $B = \text{erfc}^{-1}(2\alpha)$ and the scaling function $h(z)$ is exactly the same as in Eq. (26).

Thus, to summarise, the gap statistics have characteristic scale $\ell_N(k) = \sqrt{D/(rk^2 \ln(N/2))}$ when $k = O(1)$ and $\lambda_N(\alpha) = \sqrt{4\pi D/r} e^{B^2}/N$ for $k = \alpha N$, which are thus different. Indeed, the gap near the extreme typically scales as $1/\sqrt{\ln N}$, which is much larger than the scale $1/N$ in the bulk. But remarkably, the associated scaling function $h(z)$

in Eq. (26) is exactly the same in both cases and hence is completely universal. As discussed in the main text, this is very different from the log-gas case in random matrix theory. Finally, one can easily verify that the two regimes smoothly match with each other as $\alpha = k/N \rightarrow 0$. To show this, we need to show that $\ell_N(k)$ in Eq. (25) and $\lambda_N(\alpha)$ in Eq. (35) coincide with each other to leading order for large N when one sets $\alpha = k/N$ in $\lambda_N(\alpha)$. Noticing that, by definition, $\operatorname{erfc}(B) = 2\alpha = 2k/N$, we see that, as N becomes large, B also becomes large. We then use the leading asymptotic behavior $\operatorname{erfc}(B) \approx \frac{e^{-B^2}}{B\sqrt{\pi}}$ to write

$$\frac{e^{-B^2}}{B\sqrt{\pi}} \approx \frac{2k}{N}. \quad (36)$$

This indicates that, to leading order for large N ,

$$B \approx \sqrt{\ln(N/2)}. \quad (37)$$

Using these expressions in $\lambda_N(\alpha)$ in Eq. (35) we get

$$\lambda_N(\alpha) = \sqrt{\frac{4\pi D}{r}} \frac{e^{B^2}}{N} \approx \sqrt{\frac{D}{r}} \frac{1}{k^2 B}, \quad (38)$$

where we used (36). Finally, using (37), we see that $\lambda_N(\alpha = k/N)$ indeed coincides with $\ell_N(k)$ in Eq. (25).

C. Asymptotic behavior of the scaling function $h(z)$

We derive the asymptotic behaviors of the scaling function $h(z)$ given in Eq. (26), namely

$$h(z) = 2 \int_0^\infty du e^{-u^2 - \frac{z}{u}}. \quad (39)$$

For $z \rightarrow 0$, one trivially has $h(0) = \sqrt{\pi}$. However, one sees that the function is not analytic near $z = 0$ since a naive Taylor expansion of the integrand in powers of z yields diverging integrals. One can actually split the integral into two intervals $[0, z]$ and $[z, +\infty)$. The contribution from the first interval is linear in z for small z . The leading singular correction comes from the second interval where we can expand $e^{-z/u}$ in powers of z . The first term gives $\sqrt{\pi}$ as $z \rightarrow 0$, the second term behaves as $-2z \int_z^\infty e^{-u^2}/u$, which to leading order for small z behaves as $2z \ln z$. Hence, for small z we get

$$h(z) = \sqrt{\pi} + 2z \ln z + O(z). \quad (40)$$

The large z behavior can be obtained easily by a standard saddle point method (we do not provide details here). In summary, the asymptotic behaviors of $h(z)$ are given by

$$h(z) \approx \begin{cases} \sqrt{\pi} + 2z \ln z & , \quad z \rightarrow 0 \\ 2\sqrt{\frac{\pi}{3}} \exp\left(-3\left(\frac{z}{2}\right)^{2/3}\right) & , \quad z \rightarrow \infty. \end{cases} \quad (41)$$

Thus the universal scaling function $h(z)$ has rather nontrivial asymptotic behaviors. Its derivatives diverges logarithmically at $z = 0$ and it has a stretched exponential tail for large z , with a stretching exponent $2/3$. A plot of this function is shown in Fig. 2b in the main text.

Thus, summarizing the distribution of d_k for $k = O(1)$ and for $k = O(N)$, we obtain

$$P(d_k) \approx \begin{cases} \frac{1}{\ell_N(k)} h\left(\frac{f_k}{\ell_N(k)}\right) & \text{for } k = O(1) \quad \text{and} \quad \ell_N(k) = \sqrt{\frac{D}{r k^2 \ln(N/2)}} \\ \frac{1}{\lambda_N(\alpha)} h\left(\frac{M_k}{\lambda_N(\alpha)}\right) & \text{for } k = O(N) \quad \text{and} \quad \lambda_N(\alpha) = \sqrt{\frac{4\pi D}{r}} \frac{e^{B^2}}{N}, \end{cases} \quad (42)$$

where $B = \operatorname{erfc}^{-1}(\alpha)$ and the universal scaling function, independent of k , is given in Eq. (39).

III. NUMERICAL SIMULATIONS

We briefly outline here the method of numerical simulations used in the main text. We consider N Brownian particles on a line, each with the same diffusion constant D . They all start at the origin at $t = 0$. Let $x_i(t)$ denote the position of the i -th particle at time t . These positions evolve by the following stochastic rule. In a small time Δt

$$x_i(t + \Delta t) = \begin{cases} 0 & \text{with prob. } r\Delta t, \\ x_i(t) + \sqrt{2D\Delta t}\eta_i(t) & \text{with prob. } 1 - r\Delta t \end{cases} \quad (43)$$

where r is the resetting rate and $\eta_i(t)$ are IID Gaussian random variables with zero mean and unit variance. Note that this equation holds for all i , in particular the first line in Eq. (43) shows that when a resetting event happens, the particles are all simultaneously reset to the origin. This gives us the trajectories of the gas of N particles, i.e., the vector $\{x_1(t), x_2(t), \dots, x_N(t)\}$ at all time t . In the long time limit, the distribution of $\{x_1(t), x_2(t), \dots, x_N(t)\}$ approaches a non-equilibrium stationary state $P_{\text{stat}}[\{x_i\}]$ as given in Eq. (3) of the main text. Numerically, we keep track of this trajectory vector $\{x_1(t), x_2(t), \dots, x_N(t)\}$ and measure different observables from it in the stationary state. The results presented in the main text in Fig. 2 are then obtained by averaging over 10^5 samples. We used the parameter values $D = 0.5$ and $r = 1$.

-
- [1] H. A. David, H. N. Nagaraja, *Order statistics*, John Wiley & Sons (2004).
 - [2] G. Schehr, S. N. Majumdar, In *First-passage phenomena and their applications*, Eds. R. Metzler, G. Oshanin, and S. Redner, (pp. 226-251), (World Scientific, Singapore, 2014), arXiv:1305.0639
 - [3] S. N. Majumdar, A. Pal, G. Schehr, *Phys. Rep.* **840**, 1 (2020)